23

Solidification of Polypropylene Under Processing Conditions – Relevance of Cooling Rate, Pressure and Molecular Parameters

Valerio Brucato and Vincenzo La Carrubba
Dipartimento di Ingegneria Chimica, Gestionale, Informatica, Meccanica Università di Palermo, Palermo
Italy

1. Introduction

Polymer transformation processes are based on a detailed knowledge of material behaviour under extreme conditions that are very far from the usual conditions normally available in the scientific literature. In industrial processing, for instance, materials are subjected to high pressure, high shear (and/or elongational) rates and high thermal gradients. These conditions lead often to non-equilibrium conformational states, which turn out to be very hard to describe using classical approaches. Moreover, it is easy to understand that the analysis of the relationships between the processing conditions and the morphology developed is a crucial point for the characterisation of plastic materials. If the material under investigation is a semicrystalline polymer, the analysis becomes still more complex by crystallisation phenomena, that need to be properly described and quantified. Furthermore, the lack of significant information regarding the influence of processing conditions on crystallization kinetics restricts the possibilities of modelling and simulating the industrial material transformation processes, indicating that the development of a model, capable of describing polymer behaviour under drastic solidification conditions is a very complex task.

However, new innovative approaches can lead to a relevant answer to these scientific and technological tasks, as shown by some recent developments in polymer solidification analysis (Ding & Spruiell, 1996, Eder and Janeschitz-Kriegl, 1997, Brucato et al., 2002) under realistic processing conditions. These approaches are based on model experiments, emulating some processing condition and trying to identify and isolate the state variable(s) governing the process.

So far, due to the experimental difficulties, the study of polymer structure development under processing conditions has been mainly performed using conventional techniques such as dilatometry (Leute et al., 1976, Zoller, 1979, He & Zoller, 1994) and differential scanning calorimetry (Duoillard et al., 1993, Fann et al., 1998, Liangbin et al., 2000). Investigations made using these techniques normally involve experiments under isothermal conditions. However experiments under non isothermal conditions have been limited to cooling rates several orders of magnitude lower than those experienced in industrial processes, which often lead to quite different structures and properties. Finally, in the last

years, experiments revealing the crystallinity evolution by measures of crossing light scattering, have been conducted at intermediate cooling rate (Strobl, 1997, Piccarolo, 1992).

For the sake of completeness, it should be conceded that the complexity of the investigation concerning polymer solidification under processing conditions is even greater if the wide latitude of morphologies achievable is considered, especially when dealing with semicrystalline polymers. This would have to take into account also the complexity introduced by the presence of the crystallization process (Eder & Janeschitz-Kriegl, 1997).

Generally speaking, polymer crystallization under processing conditions cannot be considered an "equilibrium" phenomenon, since it is not possible to separate the thermodynamics effects on the processes from the kinetic ones. Furthermore, crystallization of polymeric materials is always limited by molecular mobility, and very often leads to metastable phases, as recently shown by Strobl (Strobl, 1997). Further evidences of the formation of metastable phases under drastic conditions (high cooling rates and/or high deformation rates) have been widely reported for iPP (Piccarolo, 1992, Piccarolo et al., 1992a). Choi and White (Choi & White, 2000) described structure development of melt spun iPP thin filaments, obtaining conditions under which different crystalline forms of iPP were obtained as a function of cooling rate and spinline stresses. On the basis of their experimental results together with many others available in literature, the authors have constructed a diagram, which indicates the crystalline states formed at different cooling rates in isotropic quiescent conditions. Continuous Cooling Transformation curves (CCT) have been reported on that diagram. According to the authors, at low cooling rates and high stresses, the monoclinic a-structure was formed, whereas at high cooling rates and low stresses a large pseudo-hexagonal/smectic ("mesophase") region was evident.

The formation of metastable phases normally takes place in a cooling rate range not achievable using the conventional techniques mentioned above; nevertheless it is worth reminding that the behaviour of a given semi-crystalline polymer is greatly influenced by the relative amount of the constitutive phases. From this general background the lack of literature data in this particular field of investigation should not be surprising, due to the complexity of the subject involved. The major task to tackle is, probably, to identify the rationale behind the multiform behaviour observed in polymer solidification, with the aim of finding the basic functional relationships governing the whole phenomenon. Therefore a possible approach, along this general framework, consists of designing and setting-up model experiments that could help to isolate and study the influence of some experimental variables on the final properties of the polymer, including its morphology. Thus a systematic investigation on polymer solidification under processing conditions should start on the separate study of the influence of flow, pressure and temperature on crystallization.

Due to experimental difficulties, there are only a few reports on the role of pressure in polymer crystallization, especially concerning its influence on the mechanical and physical properties. Moreover, the majority of studies made at high pressure have concentrated only on one polymer, polyethylene, dealing with the formation of extended chain crystals, as shown by Wunderlich and coworkers (Wunderlich & Arakaw, 1964, Geil et al., 1964, Tchizmakov, 1976, Wunderlich, 1973, 1976, 1980, Wunderlich & Davison, 1969, Kovarskii, 1994). The pressure associated with such investigations tends to be extremely high (typically 500 MPa) with respect to the pressures normally used in industrial processes. Furthermore, the experimental conditions normally investigated were quasi-isothermal. This implies that

the obtained results may not be applied to conventional polymer processing, involving very high thermal gradients.

The purpose of this chapter is to provide a general experimental route for studying the crystallization behaviour of isotactic polypropylene under high cooling rates and pressure.

In this respect, two complementary devices were used. The first involves a special equipment that has been developed, and widely tested, to quench polymeric samples at atmospheric pressure in a wide range of cooling rates (from 0.1 up to ca 2000 °C/s) under quiescent conditions and with the use of which it has been possible to collect much information about the influence of cooling rate on the final properties. The second was an innovative equipment specifically designed to evaluate the combined effect of typical injection moulding pressures (up to 40 MPa) and temperature gradients (up to a maximum of ca 100 °C/s), with the aid of a modified injection moulding machine. The results show that the influence of pressure on polymer crystallization is not as obvious as one may expect. An increase of cooling rate generally determines a transition from crystalline to non-crystalline (or pseudo-crystalline) structures. As for the influence of pressure, in iPP an increase in pressure results into a decrease of crystallinity, owing to kinetic factors, such decreased mobility related to the increased Tg.

In the last part of the chapter, a discussion on the influence of molecular parameters on the crystallization kinetics of iPP under processing conditions is presented. As a matter of fact, the crystalline structure of iPP quenched from the melt is affected not only by cooling rate, or generally by processing conditions, but also by molecular parameters like molecular mass (Mw) and molecular mass distribution (Mwd). Different configurations (isotacticity and head-to-tail sequences) or addition of small monomeric units and nucleating agents can also influence the final structure (De Rosa et al., 2005, Foresta et al., 2001, Sakurai et al., 2005, Nagasawa et al., 2005, Raab et al., 2004, Marigo et al., 2004, Elmoumni, 2005, Chen et al., 2005).

Influence of molecular weight on polymer crystallization is controversial. Stem length indeed interferes with entanglement density, thus determining a rate controlled segregation regime of topological constraints in non crystalline regions. Very low molecular weight tails of the distribution are shown to positively affect crystallization kinetics although their thermodynamic action should not favour perfection of crystallites (Strobl, 1997).

It is known from the literature that crystallization kinetics of semicrystalline polymers is influenced by the presence of contaminants. The main effect of the addition of a nucleating agent is an increase of the final crystallinity level together with a higher final density and a finer and homogeneous crystal size distribution. This typical effect of enhancement of the overall crystallization kinetics allows one to infer that crystallization kinetics are nucleation-controlled, being the nucleation step the rate determining one whilst the growth rate remains almost unaffected (Nagasawa, 2005, Raab, 2004).

On the other hand, the incorporation of a small content of ethylene units in the polypropylene chains has an influence on the regularity of the molecular structure. In fact, a change in tacticity induced by the shortening of isotactic sequences was observed (Zimmermann, 1993). Although this has a negative influence on crystallisation kinetics, an opposite effect should come from the enhanced mobility due to the presence of the ethylene sequences. As a result of these counteracting effects, a relatively narrow window of cooling rates exists in which an enhancement of crystallization kinetics sets in (Foresta et al., 2001).

A better understanding of the relation between processing and properties can be achieved if the absolute crystallinity during transformation can be predicted as a function of processing conditions. This prediction has to be supported by a crystallization kinetics model; here a modified two-phase non-isothermal form of the Kolmogoroff-Avrami-Evans model was used to describe the crystallization kinetics (Avrami, 1939, 1940, 1941, Evans, 1945, La Carrubba et al., 2002a, Brucato et al., 1993). The main purpose of this analysis is to underline the relevance of thermal history resulting from various cooling conditions on the crystallization kinetics of different grades of iPP containing various additives such as nucleating agents and small content of ethylene.

More specifically, the discussion attempts to identify relevant material parameters determining quiescent non isothermal crystallization kinetics simulating polymer solidification under processing conditions. One has obviously to cope with commercially relevant grades, which implies constraints in the span they cover. Therefore limitations arise not only due to the intrinsic poor significance of material parameters to crystallization kinetics but also owing to the limitation on the grades one can recover on the market. Finally, one of the main issues of this part of the chapter is the appropriate comparison among the investigated iPP samples in order to outline, when possible, the influence on the crystallization kinetics of average molecular mass, molecular-mass distribution, isotacticity, copolymerization with small amount of ethylene units and the addition of nucleants.

2. Description of the experimental procedure

2.1 Rapid cooling experiment at atmospheric pressure

A schematic drawing of the experimental set-up is shown in **fig. 1 a**. The sample, properly enveloped in a thin aluminium foil, so as to avoid leakage of material while in the molten state, (see **fig. 1 b**), and sandwiched between two identical flat metallic slabs, is heated to a suitable high temperature in a nitrogen fluxed environment.

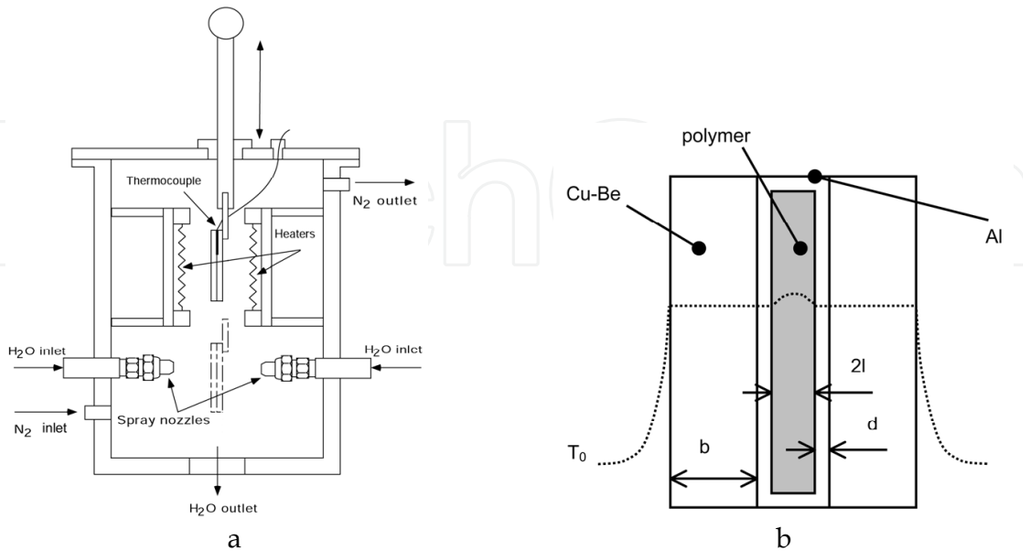

Fig. 1. a. Scheme of the experimental set-up for quench experiments; b. Sample assembly and temperature profiles. b=1-2 mm; l=50-100 μm; d=10 μm

A fast response, 12.5 μm thick (Omega type CO2), thermocouple buried inside one of the slabs allows to record the whole thermal history by a data acquisition system.

A Cu-Be alloy was chosen for the production of the metallic slabs, owing to its high Young's Modulus coupled with a high thermal conductivity (see Goodfellow Catalogue, 1996).

After keeping the sample system at a temperature above the equilibrium melting temperature for a time sufficient to erase memory effects (Alfonso & Ziabicki, 1995, Ziabicki & Alfonso, 1994), the sample assembly was moved to the lower zone of the container where it was quenched by spraying a cooling fluid on both faces through two identical nozzles positioned symmetrically opposite to each face of the sample assembly (**fig. 1a**).

The cooling rate was varied by changing the cooling fluid, its flow rate and temperature, or by changing the thickness of the sample assembly. However, the coolant temperature may not be crucial if it is sufficiently lower than the polymer solidification temperature.

Once the sample reached the final temperature it was immediately removed from the sample assembly and kept at low temperature (-30°C) before further characterization.

Three typical thermal histories (i.e. variation of temperature with time) obtained using this device are shown in **fig. 2**. Results of an extended set of experiments are reported in **fig. 3** as recorded variation of cooling rate with sample temperature. The data in **fig. 3** represent the range of variation of cooling rate covering five orders of magnitude (0.01-1000°C/s). This result is particularly significant when compared to standard DTA or DSC runs which cover only the lowest two decades of this cooling rate range (0.01-1°C/s). It is worth noting that for crystallization kinetics the high cooling rates are very informative, especially for fast crystallizing polymers, such as polyolefins. However, the high cooling rates severely restrict the possibility to detect the structural modifications taking place during solidification. The latter is the main constraint with respect to the real-time information provided by DTA and DSC measurements.

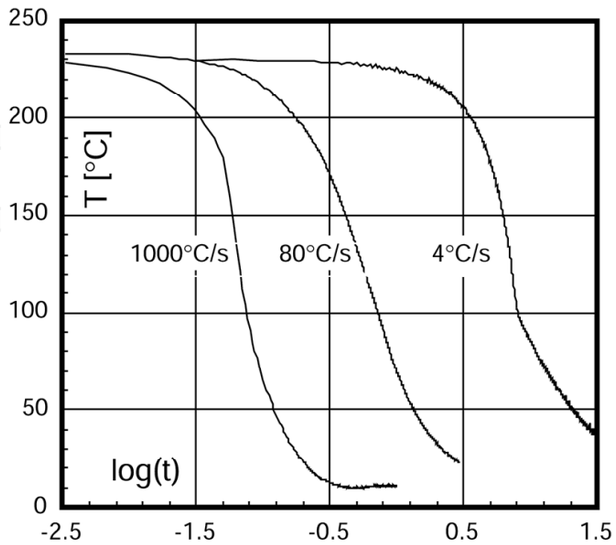

Fig. 2. Typical thermal histories for spray cooled samples

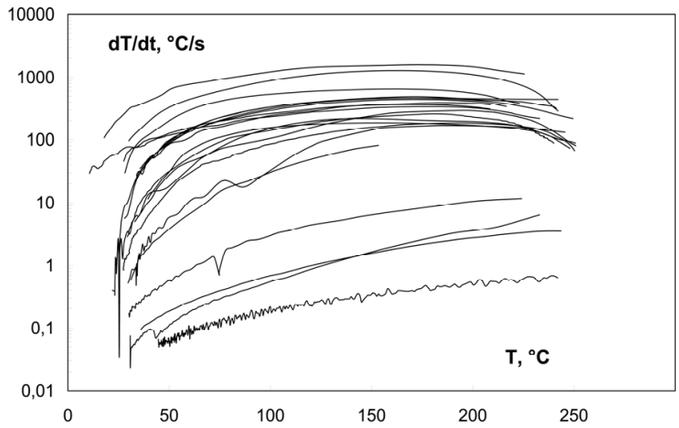

Fig. 3. Typical experimental cooling rates variation with sample temperature

With respect to the thermal histories in **fig. 2**, one will note that there is no temperature plateau associated with crystallization, the process occurring during cooling. This is due to the fact that temperature was measured on the metal slabs and not in the bulk of the polymer sample, albeit the latter has a negligible mass and volume relative to the size of the metal slabs. Furthermore, the very high heat flux to which the polymer was subjected masks the effect of the latent heat of crystallization. So, only the temperature-time history is recorded and, therefore, at the end of the cooling process one gets a thin polymeric film with a known thermal history. Sample structure depends on its thermal history and this relationship can be experimentally assessed if the "length scale" of structural features developed is small compared to the sample thickness and if the final structural features are uniform throughout the whole sample (Titomanlio et al., 1997, Titomanlio et al., 1988a, Titomanlio et al., 1988b). The sample homogeneity is thus crucial to the method envisaged since the recorded thermal history is the only available information for the determination of the final structure of the sample. The proposed model experiment is addressed to design a method for the characterization of the non-isothermal solidification behaviour encompassing typical cooling conditions of polymer processing. Only temperature history determines the structure formed as the melt solidification takes place in quiescent conditions. A discussion on the temperature distribution in a mono-dimensional heat exchange regime and the evaluation of structure distribution obtained along the thickness follows.

2.1.1 Cooling mechanism

We will consider now the effect of the applied heat flux on the temperature distribution of the metal in the sample assembly. Later in the next section the temperature distribution across the sample in contact with the metal will be examined.

The shape of the temperature profile in a flat slab having the following characteristics, thickness $2b$ and thermal conductivity k, and conditions, initial temperature T_i, suddenly exposed to a cooling medium at temperature T_0 and draining heat from the slab with a heat exchange coefficient h it is determined by the dimentionless Biot number:

$$Biot = h \times b / k \tag{1a}$$

For our experimental conditions the highest value of *Biot* number is estimated to be 0.3. Although this value does not fulfil the classical requirements for a flat temperature profile distribution within the slab (which requires *Biot* < *0.1*), the slab "cooling time" is practically unaffected by slab conductivity, therefore the so-called "regular regime" conditions still apply (Isachenko et al., 1987). In other words, the maximum Biot number for achieving a flat temperature profile is:

$$\mathrm{Biot}_{\max}=0.1 \tag{1b}$$

On the other hand, an estimate of the response time of the slabs assembly can be easily taken as the time needed for the mid plane to undergo 99% of a sudden drop of the wall temperature. The solution of such transient heat conduction problem gives the characteristic time τ_R as (Carslaw et al., 1986, Bird et al., 1960):

$$\tau_R = 2b^2 / \alpha \tag{2}$$

Where α and b are thermal diffusivity and half thickness of the slab respectively. Using the values of $\alpha = 2.6\ 10^{-5}$ m^2/s (copper-beryllium 2% alloy – Goodfellow Catalogue, 1996) and b=0.001m in **equation (2)** gives τ_R =0.07 s. Note that the fastest cooling rate in our experiments has a characteristic time τ_A =0.33 s, which is about five times τ_R. Furthermore, since the real wall boundary thermal condition on the slab is not as sharp as the assumed stepwise drop of the wall temperature, the heat conduction inside the assembly does not affect the cooling history to any appreciable extent. Applying a more realistic boundary condition, i.e. a wall temperature depending on the heat flux, does not lead to a sudden wall temperature drop, and the ratio τ_A / τ_R becomes larger.

In the experiments water sprays were used to drain heat from the slab, therefore the associated heat transfer coefficient depends very much on the flow rate of the cooling medium, as shown in **figs. 4 a-b**. Here the heat flux was evaluated according to the lumped temperature energy balance on a slab of volume *V=Sx2b*, having a heat capacity c_p and density ρ:

$$\rho c_p V\, dT / dt = h\, 2S\,(T_0 - T) = -h2S\left(T - T_0\right)$$

$$dT / dt = (T_0 - T) / \tau_l = -\left(T - T_0\right) / \tau_l \qquad \tau_l = \rho c_p b / h \tag{3}$$

Where *S* is the slab surface, *h* heat transfer coefficient, T_0 the coolant temperature and *T* the lumped sample temperature. By assuming that the heat exchange coefficient *h* is constant, then slope of the cooling rate versus temperature curve is also constant, while the slab temperature decays exponentially with time.

Fig. 4a shows that below the maximum and using smaller nozzles, giving lower mass flow rates, there are two heat transfer regimes separated by the Leidenfrost temperature, i.e. by the onset of temperature for the production of a boiling layer nucleated by the surface of the slab. In **fig. 4b** the increase of coolant mass flow rate results in the disappearance of the Leidenfrost temperature and brings about an extension of the linear dependence of heat flux to a higher temperature range up to the maximum (Ciofalo et al., 1998).

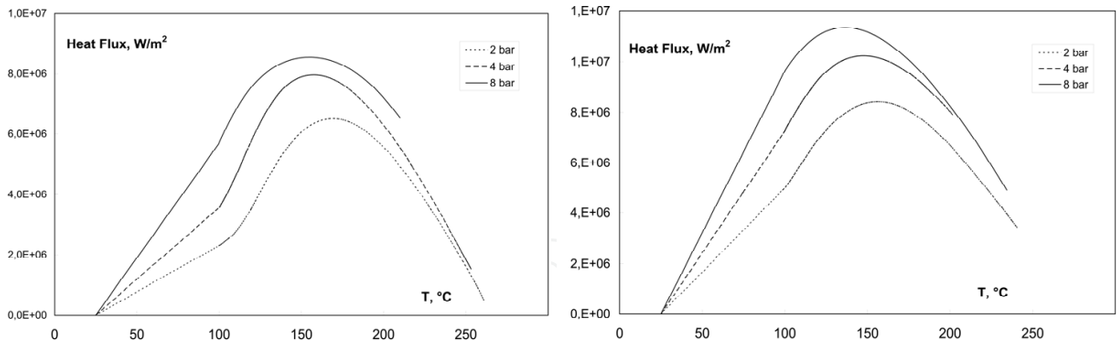

a b

Fig. 4. Heat Flux variation with sample assembly temperature for two different (a, small nozzles and b, large nozzles) spray nozzles

As long as the heat flux depends on temperature linearly, a constant heat transfer coefficient can be successfully used. This condition is well identified in the low driving force (low temperature difference) region. This result can be understood considering that the heat transfer of convection induced by the liquid drops impacting onto the solid surface is similar to that of nucleated boiling, since it promotes the renewal of the liquid layer close to the solid surface. Indeed the two mechanisms take place in parallel and the spray cooling effectiveness can be varied by changing the mass flow rate of the coolant and, at high values of the mass flow rate, the same value of the heat exchange coefficient is attained in a temperature range spanning from ambient temperature to about 150°C. This last point is particularly relevant for fast crystallizing polymers since high heat transfer coefficients are required at low temperatures to quench them effectively, as in the case of iPP.

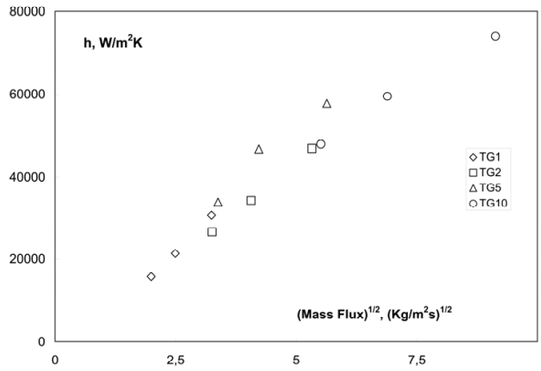

Fig. 5. Heat exchange coefficient vs. coolant mass flux for four different spray nozzles

The relationship between the liquid convection heat transfer coefficient, *h*, and the mass flow rate is summarized in **fig. 5** for all the nozzles used in this work**.** Within an error of ±10% there is a square root dependence of *h* on mass flow rate (Ciofalo et al., 1998).

The time constant, τ_l , obtained from **equation (3),** attains a minimum value of about 0.05 s. A comparison of the values of $5 \times \tau_l$ and τ_R (98.5% of the overall temperature drop) shows

that the driving force (i.e. the temperature drop) is larger in the fluid than in the Cu-Be slab, i.e. the heat transfer is mainly controlled by the fluid heat transfer. At the same time and the definition of τ_l suggests that another way to change linearly the slope of the cooling curves of **figs. 4 a-b** is by modifying the slab thickness. Moreover **equations (2)** and **(3)** show that the ratio τ_l / τ_R is proportional to the inverse of the thickness, suggesting that one should use the thinnest possible slab to achieve a more uniform temperature distribution through the thickness.

In principle the time constant, τ_l, drawn from **figs. 4 a-b** could be used as a parameter to rigorously identify the overall cooling process (Ding & Spruiell, 1996). When the solidification temperature of the polymer falls in a range in which there is a change of the heat transfer regime, the heat transfer coefficient will also change with temperature while the use of τ_l becomes meaningless, as it is no longer constant. On the other hand, the value of τ_l changes slightly when the temperature range where solidification takes place is quite narrow (of the order of 10°C). Although an average value of τ_l could be used, it is preferred to use an equivalent parameter to identify the cooling process, which is the average cooling rate in the range of temperatures within which the polymer solidifies (Brucato et al., 2002, Piccarolo, 1992, Piccarolo et al., 1992a, Piccarolo et al., 1992b, Brucato et al., 1991a, Brucato et al., 1991b, Piccarolo et al. 1992, Piccarolo et al., 1996, Brucato et al., 2009). This parameter, indeed, imposes not only the experimental time to be constant, but also the characteristic range of temperatures in which a given polymer solidifies. For iPP, the average cooling rates at around 70°C (Piccarolo et al., 1992a, Brucato et al., 2002, Brucato et al., 2009) has been chosen, as the parameters characterizing the cooling effectiveness for that polymer. Although this is a semi-quantitative measure of cooling effectiveness, the whole thermal history is available to compare experimental results with predictions from non isothermal kinetic models (Piccarolo et al., 1992a, Brucato et al., 1991a). Furthermore, if the kinetic constant vs. temperature relationship is mapped to the temperature vs. time profile, it is clear that an underestimate of the effective cooling rate is obtained only at low cooling rates. With an exponential temperature decay most of the solidification takes place around the maximum of the kinetic constant, i.e. in the chosen temperature interval.

2.1.2 Temperature distribution in the polymer sample

The solution of **equation (3)**, introducing the dimensionless temperature of the Cu-Be slab Θ_{Cu} with boundary conditions $T=T_i$ for $t=0$ and constant heat exchange coefficient h, is:

$$\Theta_{Cu} = \exp\left(-t / \tau_l\right) \tag{4}$$

where T_i and T_0 are the initial and final temperatures respectively.

If sample thickness is very small compared to that of the slab, **equation (4),** representing the time dependence of the slab temperature (i.e. the temperature at the sample surface), becomes an exponential decay equation with a time constant defined by **equation (3)**. Furthermore, in the case of very high cooling rates, this dependence of temperature on time extends to high temperatures. The smallest characteristic times are then obtained in the largest temperature range.

An estimate of the temperature profile in the polymer sample under these cooling conditions is, therefore, conservative and may well provide a case for achieving the maximum cooling rates with this technique, aiming to achieve a homogeneous thermal history throughout the entire sample thickness. As it has been previously pointed out, this condition must be satisfied in order to devise a direct relationship between structure obtained and the associated thermal history.

The temperature distribution in the solid polymer sample can well be approximated by the Fourier equation for transient heat conduction within a medium of constant thermal diffusivity, i.e.

$$dT_{pol} / dt = \alpha \times \partial^2 T_{pol} / \partial x^2 \tag{5a}$$

Or, in dimensionless form, i.e.

$$d\Theta_{pol} / dFo = \partial^2 \Theta_{pol} / \partial \xi^2 \tag{5b}$$

Where: $\xi = x / l$, dimensionless half depth; l =slab half depth; $Fo = \alpha t / l^2$ =Fuorier number;

With boundary conditions:

1. When $Fo = 0$ then $\Theta_{pol} = 0 \quad \forall \xi$ (flat temperature profile before cooling);
2. For $\xi = 0$, $\partial \Theta_{pol} / \partial \xi = 0 \ \forall Fo \geq 0$ (symmetry.)

The cooled wall boundary condition is an exponential decay of temperature according to experimental observation:

3. For $\xi = 1$, $\Theta_{pol} = \phi(Fo) = \exp(-t / \tau) \ \forall Fo \geq 0$ (τ = exponential time constant, s) (6)

However, **Equation (5.b)** neglects the heat generated by the latent heat of crystallization. An analytic solution of **equation (5.b)** with the boundary conditions given by **equations (6)** is provided in some texts (Luikov, 1980), i.e.

$$\Theta_{pol}(\xi, Fo) = \frac{\cos\left(\xi \cdot \sqrt{Pd}\right)}{\cos\sqrt{Pd}} \cdot \exp(-Pd \cdot Fo) + \sum_{n=0}^{\infty} \frac{2\cos\left[(2n+1)\pi/2 \cdot \xi\right]}{(\pi/2 + n\pi)\sin\left[(2n+1)\pi/2\right]} \exp\left(-\mu_n^2 \cdot Fo\right) \tag{7}$$

With $\mathrm{Pd} = \mathrm{l}^2 / \alpha \cdot \tau$, *Predvotitelev* number (dimensionless time constant) and $\mu_n = \pi / 2 + n\pi$ **.**

A similar analytic solution is also provided in other texts (Carslaw & Jaeger, 1986), but (probably due to a misprint) any attempt to use the reported solution has failed.

Prediction of temperature profiles for an iPP slab (Brangrup & Immergut, 1989, van Krevelen, 1972) cooled with an exponential decay from T_i=230°C to T_0=5°C, are summarized for the case of two sample thicknesses (0.2 and 0.1 mm) in **figs. 6** and **7** respectively. The smallest time constant, $\tau_l = 0.05s$, corresponding to the fastest experiment performed, is considered. While diagrams **a)** of **figs. 6** and **7** show the calculated temperature distribution across the thickness (only half sample is considered), diagrams **b)** shows the calculated dependence of cooling rate on temperature at different sample depth along the thickness

direction. One can observe that for a sample thickness of 0.1 mm (**fig. 7**) the temperature distribution is almost flat across thickness. Significant deviations on the cooling rate versus temperature dependence are observed only at temperatures significantly higher than the range of solidification for most polymers.

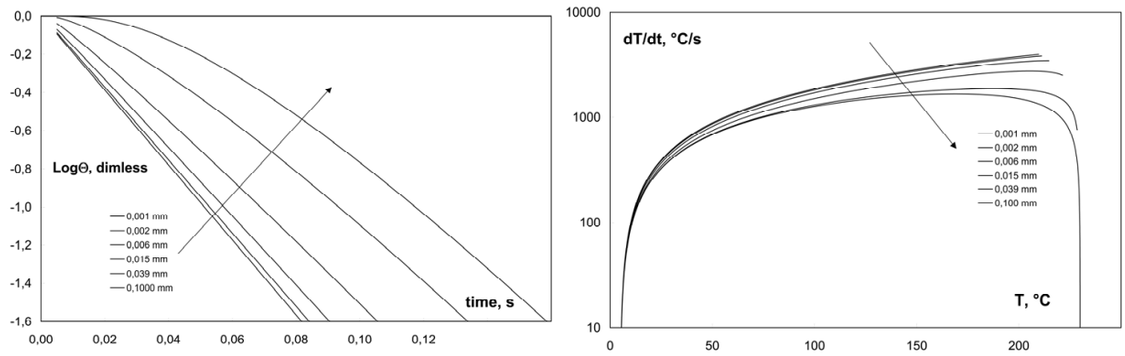

a b

Fig. 6. iPP film (half thickness=100μm) cooled from 230 to 5°C with an exponential decay with time for characteristic time τ_i=0.05s. a) calculated temperature distribution across the thickness; b) calculated cooling rate vs. temperature at different sample depth

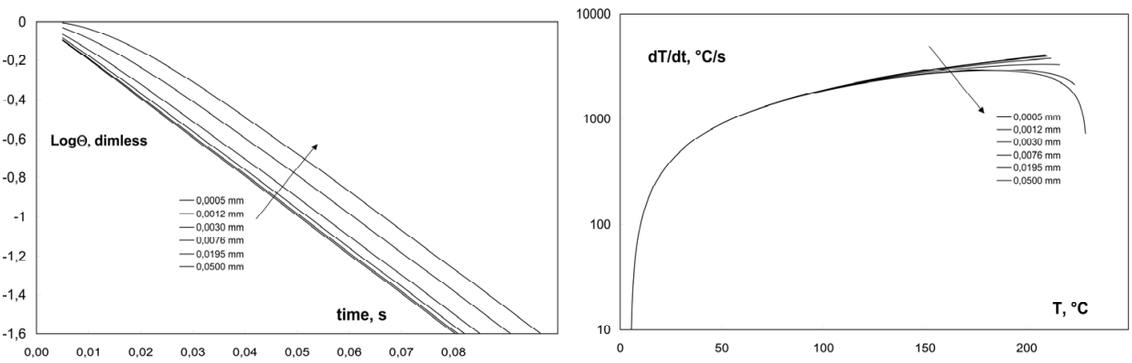

a b

Fig. 7. iPP film (half thickness=50μm) cooled from 230 to 5°C with an exponential decay with time for characteristic time τ_i=0.05s. a) calculated temperature distribution across the thickness; b) calculated cooling rate vs. temperature at different sample depth

Although this result may appear to be in contradiction with the constraint expressed by **equation (1b),** the analysis of the regimes involved in transient heat conduction, reported in advanced textbooks (Isachenko et al., 1987), provides a consistent explanation. When a solid is suddenly exposed to a coolant kept at a constant temperature T_0, the temperature profile could experience two regimes: an initial one corresponding to dissimilar temperature profiles, and a second one, called "regular", whereby the temperature profiles are almost parallel to each other and self similar at different times. Depending on the *Biot* number the second regime may also not take place and the condition *Biot<10* determines the onset of the second regime controlling the transient heat conduction for most of the cooling time. The condition expressed by **equation (1b)** may thus be seen to be more restrictive than it is

necessary, determining that the flat temperature is the controlling factor for most of the time during cooling of the solid from T_i to T_0.

In the regular regime of transient heat conduction, the onset of almost parallel temperature profiles determines a condition by which at different times the slope of the profile is the same in different sample positions, leading to the same cooling rate at the same temperature and to a correct interpretation of the calculated results reported in **figs. 6** and **7**. The temperature profile may thus be seen as a perturbation propagating from the external surface to the interior as the calculation of **figs. 6** and **7** shows. For larger sample thickness, as in **fig. 6**, although the temperature profile is not flat, the temperature distribution regime is regular and the cooling rate at lower temperatures is still almost constant throughout the sample. This is not so for cooling rates evaluated at temperatures higher than ca 80°C. On the other hand, for small sample thickness, as is shown in **figs. 7**, the heat transfer regime in the sample is always regular even at temperatures as high as 180°C.

As for the influence of the latent heat on the temperature distribution, which is neglected in **equation (5.b)**, one can observe that, although the heat of crystallization affects the temperature profile of the sample, and/or the thermal history to which it is subjected, the overall effect is only moderate. Indeed an estimate of the increase in sample temperature due to latent heat of crystallization, with the assumption that heat release takes place adiabatically, only produces maximum values of about 40°C, if the polymer sample crystallizes to the maximum allowable extent. Although this value may seem large when compared to the effect of temperature on the crystallization kinetics, it must be remembered that at low cooling rates, crystallization takes place over longer time intervals, and consequently does not affect appreciably the temperature of the sample since the heat is being released slowly. With respect to adiabatic conditions, a smaller temperature increase will, indeed, take place during cooling. Furthermore, the "heat sink" effect played by the metal slabs on the polymer film makes the temperature increase negligible. At high cooling rates, on the other hand, the heat is released in a shorter time interval, however in this case the temperature of the sample is controlled by very high heat fluxes and, consequently, the temperature is not affected very much either (Brucato et al., 2002, Brucato et al., 2000, La Carrubba, 2001). Moreover, if very drastic cooling conditions are applied, the sample only experiences a low degree of crystallization and, therefore, releases smaller amount of heat, which affects the temperature even less.

2.2 Rapid cooling under pressure

In order to evaluate the combined effect of typical injection molding pressures and temperatures, a new equipment was designed as a natural extension of the previously described apparatus. A standard Negri Bossi NB25 injection moulding machine was used as a source of molten polymer supplied at a pre determinable and maintainable pressure at which the polymer can be injected into a preheated mould cavity.

A special injection mould has been designed such that samples could be cooled at a known cooling rate and under a known pressure (Brucato et al., 2002, Brucato et al., 2000, La Carrubba, 2001). This heated mould consists of a conical cavity (the sprue), which is located in the fixed platen of the injection molding machine, coupled to a "diaphragm". The front of the cavity is sealed with a high tensile, high thermal conductivity copper-beryllium

"diaphragm", which is spray cooled on the opposite side when the quench starts. A schematic representation of the apparatus is shown in **fig. 8**. The cavity is located within a brass block where eight cartridge heaters with a total power of 2 kW are inserted. The diaphragm is located in the moving platen of the machine. The whole apparatus (cavity and Cu-Be diaphragm) has been designed in such a way that it can be placed in and removed from an injection moulding machine as a normal injection mould tool. A cooling channel, which allows the diaphragm to be spray cooled by pressurized water (at 8 bars) on one side, is also located in the mobile part. A thermocouple (type E, diam.=0.05 mm) inserted inside the diaphragm close to the wall facing the polymer sample records the thermal history during cooling, whilst a pressure sensor (type Dynisco PT46) mounted in the cavity allows measurement of pressure during the experiment. The pressure sensor and the thermocouple are connected to a data acquisition system, constituted by a National Instrument card LAB-LC coupled with an Apple–Macintosh LC computer.

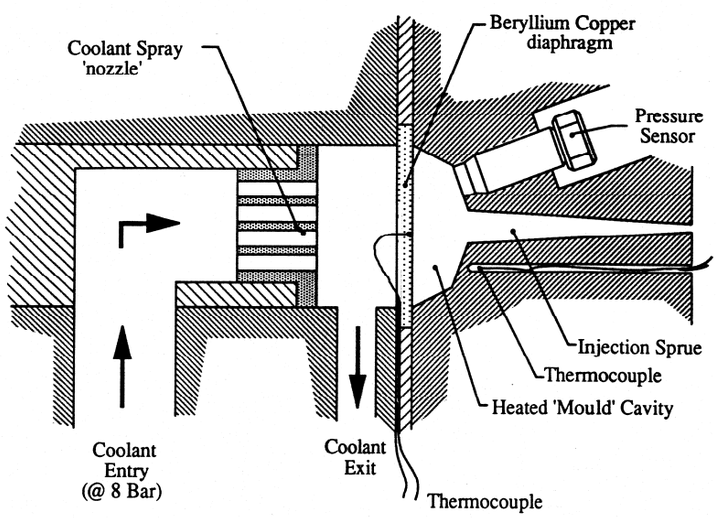

Fig. 8. Apparatus for solidification under pressure fitted to the modified injection molding machine

The experimental methodology of recording the thermal history experienced by the surface of rapidly cooled samples and then analyzing the resulting sample morphology has been adopted. Using the above described configuration, a thin layer in contact with the diaphragm solidifies under a known recorded thermal history and under a constant recorded pressure history. Internal layers of the polymer are cooled with different cooling rates, which can be calculated by solving the transient heat transfer equation **(7)**. In order to relate thermal history to the structure formed, the relationship between cooling rate evaluated at 70°C (characteristic temperatures of iPP) and depth in the sample can be calculated based on the conduction heat transfer problem **(eq. 7)**, as shown in **fig. 9**. This is a sort of "transformation function" or "mapping function", which converts the depth in the sample in an equivalent value of cooling rate, thus enabling the physical data to be mapped as a function of cooling rate rather than of the sample depth. This transformation functions allow the effect of pressure superimposed to that of cooling rate to be properly identified and quantified. Thin slices (50 to mm) microtomed across a direction parallel to the cooled

surface are then used for post-solidification characterization methods (Brucato et al., 2000, La Carrubba, 2001), being each slice characterized by a well defined cooling rate (averaged across slice thickness).

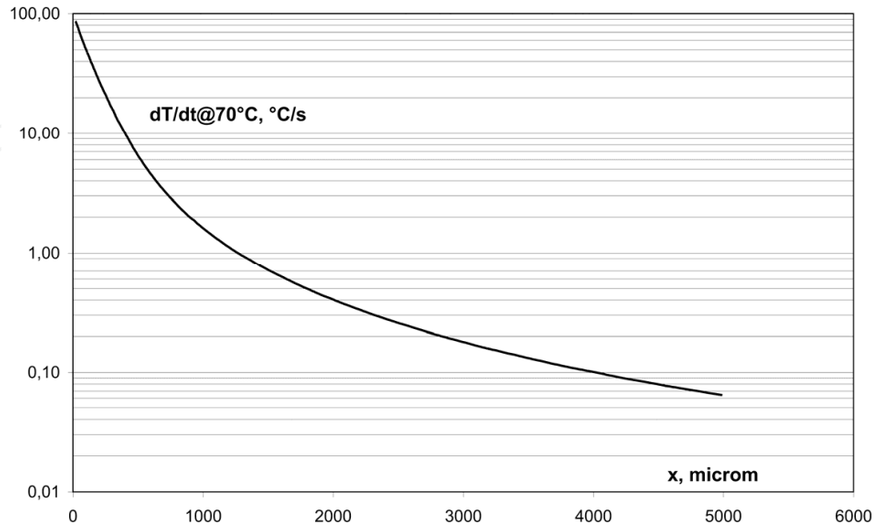

Fig. 9. Depth-Cooling Rate "mapping function"

3. Materials and characterization

Several iPP grades were analysed, with the aim of encompassing a wide latitude of crystallization behaviour and to highlight the influence of molecular parameters on iPP crystallization. The main features of the different grades of iPP tested are listed in **Table 1**.

Material name	Mw	Mwd	Xs(*)	notes
HPB	430000	6.6	2.9	
M2	208000	3.5	4.5	
M6	391000	5.6	4.6	
M7N	379000	5.3	3.4	+ Talc 1000 ppm
M9	380000	3.8	5.0	Copolymer 0.5% ethylene
M12	252000	5.4	13.9	
M14	293000	7.3	5.2	Copolymer 3.1% ethylene+DBS
M16	293000	7.3	5.2	Copolymer 3.1% ethylene
iPP1	476000	6		
iPP2	405000	26		bimodal MWD
iPP3	489000	9.7		
iPP4	481000	6.4		

Table 1. Main Characteristics of the iPPs examined. (*)Xylene soluble weight percentage

Since cooling rate in the present devices is too fast for recording any macroscopic change during the solidification process, only the final structure of the solidified sample was evaluated. The final features of the samples, analyzed by suitable macroscopic probes, such as powder Wide Angle X-Ray Diffraction (WAXD) patterns and density measurements were related to thermal history.The X-ray diffraction measurements have been performed by a Philips vertical diffractometer equipped with a Philips PW1150 generator. The Cu-Ka Nickel filtered radiation was detected in the interval 6-45°, applying steps of 0.05° in the interval 10-35° and of smaller steps of 0.2° elsewhere with a counting time of 60 s per step throughout. The gradient column technique was used for density measurements.

4. Results

4.1 Crystallization of iPP at atmospheric pressure

The results of the correlation for iPP3 between the structural features of quenched samples, assessed through the macroscopic probes cited above (WAXD and density), and thermal history, identified by the relevant cooling rate in the range of temperatures where the polymer solidifies (70°C for iPP), are shown in **figs. 10a** and **b** for density and WAXD patterns dependence on cooling rate, respectively. Such results point out the features of the proposed method of characterization already reported by the authors (Piccarolo, 1992, Brucato et al., 1993), with respect to change of structure and density with cooling rate. A broad range of density were identified as well as extreme structural features in the WAXD patterns. The WAXD patterns reported in **fig. 10b** show that at low cooling rates only the stable a monoclinic phase is observed with small amounts of the β phase, as identified by the reflection at 2θ=16.1°. The crystalline order, determined by the width of the peaks, continuously decreases on increasing cooling rate up to a point where only two broad diffraction peaks are observed, showing the presence of the so called mesomorphic phase of iPP (Corradini et al., 1986, Guerra et al., 1990). At intermediate cooling rates, the coexistence of the two phases is revealed, over a narrow range of cooling rates, by the superposition of the two broad peaks of the mesomorphic phase and the faint residues of the peaks related to the a monoclinic phase.

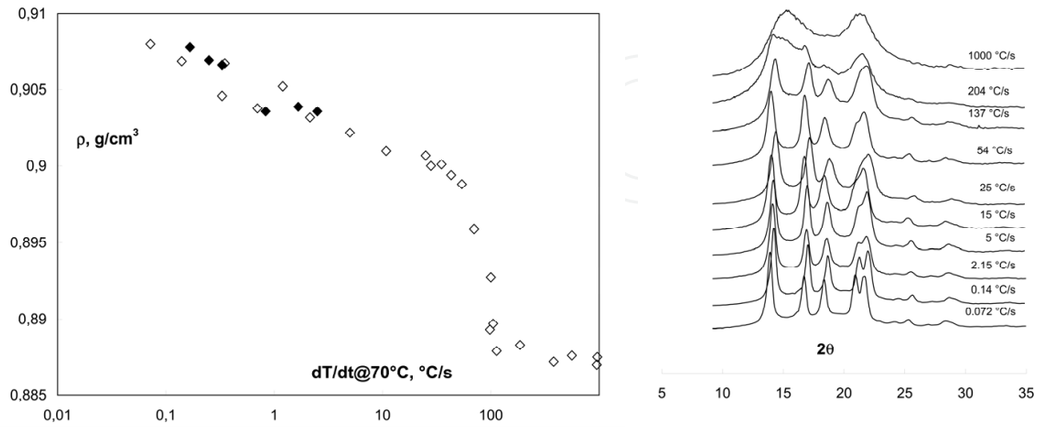

a b

Fig. 10. a. Density dependence on cooling rate (measured at 70°C) of iPP3. Open symbols: rapid cooling experiments; filled symbols: standard constant cooling rate experiments (DSC) b. Dependence of WAXD powder patterns of iPP3 on cooling rate (measured at 70 °C)

Furthermore, changes of the WAXD patterns agree with the density measurements, making the two methods consistent and comparable. Although a qualitative cross check can be made for the data in **fig. 10b**, a quantitative comparison can only be obtained by WAXD deconvolution (Martorana et al., 1997). This last has been extensively used to determine the phase content and its dependence on cooling rate. This dependence of phase content on cooling rate, in turn, has been used for the determination of non-isothermal crystallization kinetics. The model adopted was based on the crystallization kinetics of two phases competing for the transformation from melt to solid (Brucato et al., 1998, Piccarolo et al., 1992a, Brucato et al., 1993). The reason for two parallel crystallization mechanisms stems from the WAXD patterns dependence on the cooling rate. In the case of iPP, for example, the patterns show that the stable phase disappears while the mesomorphic phase content increases with increasing cooling rate.

The density versus cooling rate curve of **fig. 10.a** shows three zones characterized by different features related to the WAXD based phase content dependence on cooling rate reported in **fig. 11**:

i. At low cooling rates where only stable phases are formed, the density decreases to a small extent with the log of the cooling rate. Below ca 5°C/s a slight decrease of density is observed, related to the formation of small amount of β phase formed (Piccarolo, 1991).
ii. At the highest cooling rates, a low-density plateau is observed related to the mesomorphic phase set-in, since a limiting packing condition has been approached. The nature of the mesomorphic phase is not well known, the most acknowledged hypothesis being a packing very similar to the α-monoclinic phase but with a low range order (Corradini et al., 1986). The most significant feature of this phase, indeed, is that it transforms to the stable α-monoclinic phase upon ageing, which is relevant for the post processing behaviour of iPP. Previous studies point out that the kinetics of this transformation to be measurable only above 80°C (Struik, 1978). More recent annealing experiments, discussed elsewhere (Gerardi et al., 1997) show that such transformation can take place at much lower temperatures and can cause significant density changes.
iii. In an intermediate cooling rate range the material density shows a very high sensitivity to changes in cooling rate. In this zone the stable phase content decreases while that of the mesomorphic phase increases as the cooling rate is increased. This transition is strongly dependent on the material characteristics, e.g. nucleating agents and molecular weight (Sondegaard et al., 1997). Solidification under these intermediate cooling rates shows the effect of the competition between the a monoclinic and the mesomorphic phases in the transformation from melt to solid. The slope of the density curve in this region is a measure of the sensitivity of the crystallization kinetics towards the cooling rate for a given polymer.

To sum up, although the mapping of the structural features provides a general understanding of the relationship between the thermal history and the associated structure formed during a quenching experiment, the density dependence on cooling rate provides an immediate, quantitative information on the non isothermal crystallization behaviour of the polymer. In this respect the identification of the narrow range of cooling rates at which the transition from a monoclinic to mesomorphic phase takes place provides quantitative information on the material non-isothermal crystallization kinetics.

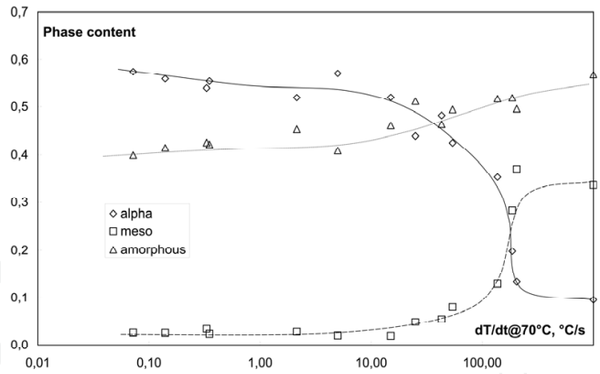

Fig. 11. WAXD deconvolution of iPP3. Phase content vs. cooling rate (measured at 70 °C)

A model-based interpretation of such transitional cooling rates performed on the crystallization kinetics parameters has been published recently (La Carrubba et al., 2002a).

4.2 Crystallization of iPP under pressure

The results of the density measurements made on iPP4 samples solidified under pressure are reported in **figs. 12.a** and **b**. Four different pressure conditions have been explored: 0.1 MPa, 8 MPa, 24 MPa, 40 MPa using two different diaphragm size 3.5 mm and 8 mm thick, (see **fig. 8**). In **fig. 12.a** is shown the density depth profile for the 3.5 mm thick diaphragm, and in **fig. 12.b** the density depth profile for the 8 mm thick diaphragm. Samples obtained with the 3.5 mm thick diaphragm were subjected to an experimental surface cooling rate (measured at 70°C -Brucato et al., 2002) of about 100°C/s. Samples solidified using the 8 mm thick diaphragm experienced a surface cooling rate of about 20°C/s. It is worth noting that the surface cooling rate depends on the coolant heat transfer and on the diaphragm thermal inertia. Changing the diaphragm thickness is, indeed, a simple and reliable way to tune the surface cooling rate (La Carrubba, 2001).

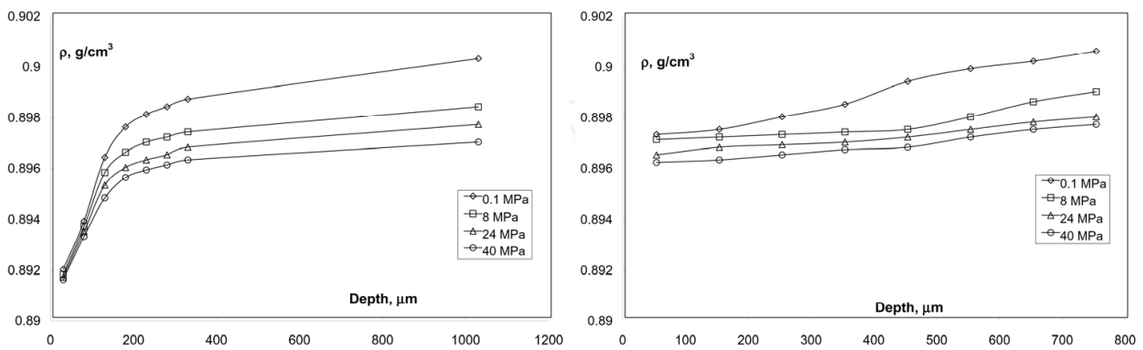

a b

Fig. 12. iPP4 Density depth profile for different solidification pressures from 0.1 to 40 MPa: a. diaphragm 3.5 mm thick; b. diaphragm 8 mm thick

The curves in **fig. 12a** and **b** show that for both experiments and at all pressures, density increases from the surface to the bulk of the sample. This behavior can be related to the

expected increase in crystallinity since the internal layers are cooled at progressively lower rates. In **fig. 12a** and **b** it is shown that the highest level of the density increase takes place in the vicinity of the surface, and that this is independent of the applied pressure.

Both **figs. 12a** and **b** show also somewhat unexpected results, in so far as a density decrease with pressure occurs at all depths in the sample. The reduction of density due to pressure is minimum at the sample surface and grows with depth. Furthermore, the majority of the density change is observed by varying the pressure from 0.1 to 8 MPa, which is quite low especially if compared with the typical pressure values used in injection moulding. This experimental result may be relevant for modeling the shrinkage and the internal stress distribution in injection molded products. Particularly important is the fact that this effect is more pronounced in the bulk of the sample.

Fig. 13 is obtained by plotting the density data in **figs. 12a** and **b** against the cooling rate calculated at 70°C by using a transient heat conduction model (equation (7). The value of the calculated cooling rate was averaged across every slice (50μm thick). The use of the transient model was also validated by overlapping the data referred to a surface cooling rate of 100 and 20 °C/s. In **fig. 13** it is also shown that at constant cooling rate the final density decreases with pressure. The same trend is obtained with respect to cooling rate, indicating that the density drop above 10-20 °C/s is independent of the solidification pressure. Finally, **fig. 13** shows that the decrease of density with pressure vanishes with increasing cooling rate, implying that the influence of pressure is more pronounced in the bulk of the sample. This is a very important information in process simulation.

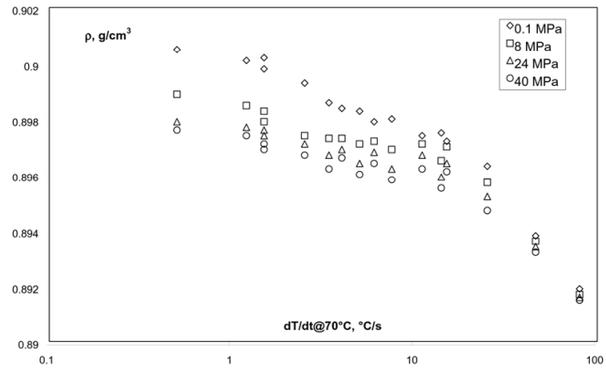

Fig. 13. iPP4 Density versus cooling rate evaluated at 70°C for different solidification pressures from 0.1 to 40 MPa

A similar pressure dependence of the density has also been observed by He and Zoller (He and Zoller, 1994) using a standard dilatometer and measuring the specific volume of this sample during crystallization from the melt. A constant slow cooling rate (2.5 °C/min) under constant pressure was used, bringing the sample back to a fixed pressure at the end of the test. It is worth noting that the majority of experiments have provided information on specific volume under pressure, whereas in our work we have measured the density at ambient pressure after solidification under pressure. He and Zoller observed an increase of specific volume with increasing crystallization pressure in the case of iPP, i.e. the specific volume in the solid phase at the end of the solidification curve is slightly higher than the one measured at the beginning of the melting curve. This behavior demonstrates that during

solidification under pressure some structural transformations take place giving final lower density values. Although He and Zoller have attempted to explain the reduction in density with the formation of the γ phase, which is less dense than the α phase, the samples in our study did not show any evidence of the presence of the γ phase (La Carrubba et al., 2000). The experiments performed by He and Zoller are in agreement with our results, which show that the final density (measured at atmospheric pressure) of samples solidified under pressure is, in fact, lower than that of the samples solidified at atmospheric pressure. We have repeated the PVT measurements on iPP and have published the results in a recent paper (La Carrubba et al., 2002b), where a comparison between specific volumes of samples crystallized at different pressures and/or cooling rates has revealed a decrease in density with increasing cooling rate and pressure. Thereafter, WAXD experiments were performed on slices cut in the transverse direction with respect to the direction of the heat flux. All experiments were performed by the synchrotron radiation source of the DESY center in Hamburg. A very long accumulation time (5 frames of 1 minute) was applied in order to achieve statistically significant results and a good reproducibility.

A qualitative analysis of the diffraction patterns has lead to the conclusion that the alpha phase content decreases on increasing cooling rate, for all the adopted pressures used (Brucato et al., 2000, La Carrubba et al., 2002a, La Carrubba et al., 2000). The data have shown that increase in pressure decreases the alpha phase content. This is better shown by WAXD data after a deconvolution procedure that has already been discussed elsewhere (Martorana et al., 1997). The program employed (implemented on MATLAB) uses a best-fitting procedure to calculate the positions and the intensity and of the alpha phase including mesomorphic phase peaks and that of the amorphous halo.

In **fig. 14** are shown plots of the phase content of the samples against pressure at four different values of cooling rates, ranging from 1.5 to 80 °C/s. A decrease of alpha phase is noticed, which is in agreement with the data from density and micro hardness measurements, showing that the change in the alpha phase content with pressure is highest within the first 10 MPa. By examining the data in **fig. 14** one notes that the decrease of the alpha phase with pressure tends to vanish when the cooling rate increases, particularly for cooling rates above 20°C/s. Additionally, the reduction of the alpha phase is mostly balanced by an increase of the mesomorphic phase content while the amorphous phase seems to be only slightly affected by pressure.

This last point is also very relevant, in so far it shows that as the main effect of pressure is to replace the alpha phase by the mesomorphic phase, leaving almost unaffected the amorphous content. It has been already shown, in fact, that the main effect of increasing the cooling rate at ambient pressure is the substitution of the alpha phase with the mesomorphic one (Piccarolo, 1992, La Carrubba et al., 2002a). In other words, the qualitative effect of pressure (at a constant cooling rate) on the final structure appears to be the same as an increase of cooling rate alone at a constant pressure (La Carrubba et al., 2000). This results is also illustrated in **fig. 15**, reporting the phase fraction, as calculated from the WAXD deconvolution of the samples, crystallized at atmospheric pressure using the rapid quenching apparatus. One can easily see how the decrease of the alpha phase with increasing cooling rate is accompanied by an increase of the mesomorphic phase (**fig. 14**). This observation is a further confirmation of the possibility to adopt a master curve approach to describe the bahaviour of iPP under pressure and high cooling rates.

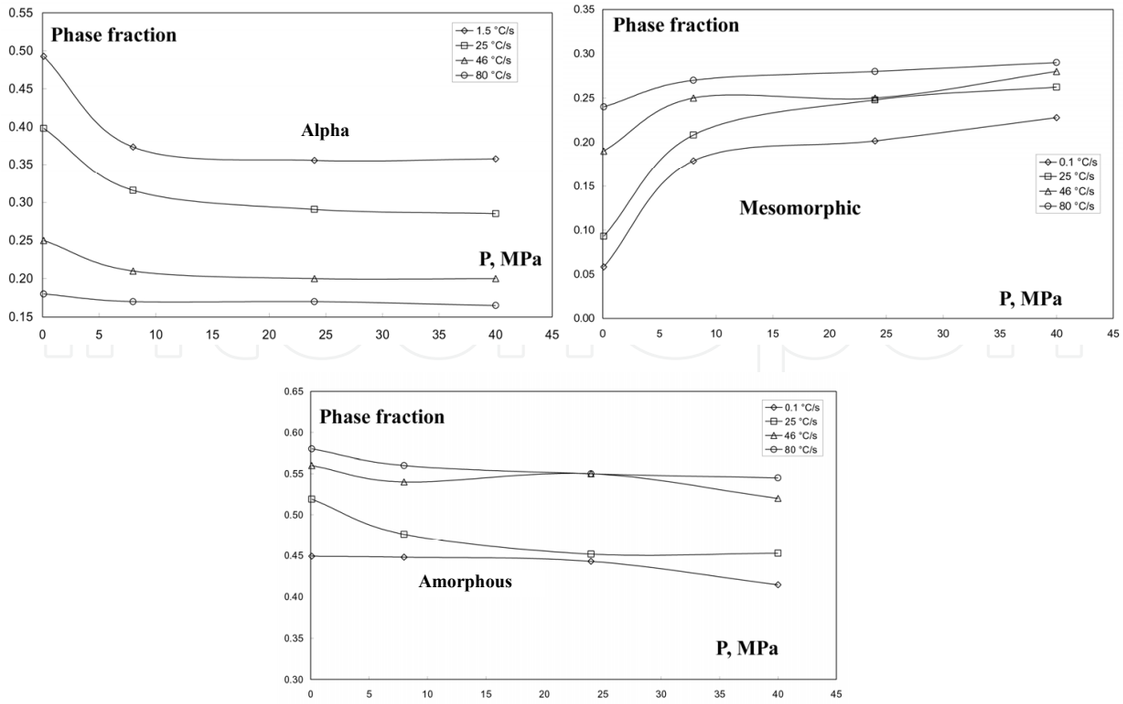

Fig. 14. Phase content of iPP4 from WAXD deconvolution as a function of pressure

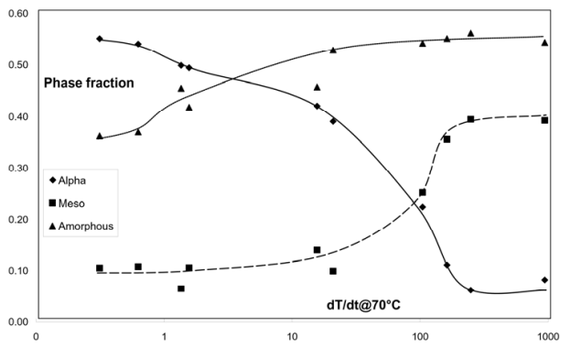

Fig. 15. WAXD deconvolution of iPP4 at 0.1 MPa, showing the phase relative content

4.3 Crystallization kinetics model

When dealing with crystallization of iPP, the numerous crystalline modifications of this material must be accounted for, since α, β or γ crystals may form upon solidification from the melt. The resulting complex frame can be simplified based on some experimental evidences, supported by several references (Foresta et al., 2001, Nagasawa et al., 2005, Raab et al., 2004, Marigo et al., 2004). As for the β phase, it basically shows up only if specific β nucleants are added, therefore for commercial non-*b*-nucleated iPP's it does not form; traces of γ form crystals are often present, but always in minor amount and in a narrow window of operating conditions (i.e. cooling rates), hence its presence is neglected without affecting the reliability of the results.

Under the aforementioned hypotheses, as two different crystalline phases are formed (α and mesomorphic), at least two kinetic processes take place simultaneously. The simplest model is a parallel of two kinetic processes non-interacting and competing for the available molten material. The kinetic equation adopted here for both processes is the non-isothermal formulation by Nakamura et al. (Nakamura et al., 1973, Nakamura et al., 1972) of the Kolmogoroff Avrami and Evans model (Avrami, 1939, 1940, 1941, Evans, 1945).

The model is based on the following equation:

$$X(t)/X_\infty = 1 - \exp\left[-E(t)\right] \tag{8}$$

Where $X(t)$ and X_∞ are the crystallized volume fraction at time t and in equilibrium conditions, respectively. For simplicity and for the sake of generalization X_∞ is here assumed to be a material constant, although it has been reported its dependence upon the crystallization history (crystal size distribution and degree of perfection, Ziabicki, 1976).

$E(t)$ is the expectancy of crystallized volume fraction if no impingement would occur. A different formulation of the model can be easily obtained by differentiation of equation (8):

$$d\xi/dt = (1-\xi)\dot{E}(t) \tag{9}$$

Where:

$$\xi = X(t)/X_\infty \tag{10}$$

Since in the case of interest two crystalline phases develop, the simplest extension of the present model is to assume that those phases grow independently in parallel, competing each other for the residual fraction of available melt. Under this hypothesis the rate equation, for the general case of m crystalline phases developing simultaneously, becomes:

$$d\xi_i/dt = (1-\textstyle\sum_i \xi_i)\dot{E}_i(t) \qquad \text{for i= 1…m} \tag{11}$$

The following function, suggested by several authors (Ziabicki, 1976, La Carrubba et al., 2002a), can be adopted for the expression of the time derivative of the expectancy, leading to a rate equation proportional to the fraction of untransformed material times the current value of the kinetic constant, in which nucleation and growth rates have been lumped together (nucleation and growth are therefore isokinetic):

$$d\xi_i/dt = (1-\textstyle\sum_i \xi_i) n_i \ln 2 \left[\int_0^t K_i(T)ds\right]^{n_i-1} K_i(T) \qquad \text{i= 1…m} \tag{12}$$

The form adopted in equation (12) for the time derivative of the expectancy reduces to the classical *Avrami* form, with a dimensionality index n_i for the i^{th} phase, if an isothermal experiment is considered. As for the dependence of the rate constant K_i on temperature, the simplest expression that one can consider is a Gaussian shaped curve:

$$K_i(T) = K_{0,i} \exp\left[-4\ln 2\left(T - T_{\max,i}\right)^2 \cdot D_i^{-2}\right] \qquad \text{i= 1…m} \tag{13}$$

where D_i, $T_{\max,i}$ and $K_{0,i}$ are the half width, the temperature where the maximum of K_i is attained and the maximum value of K_i itself, respectively (Ziabicki, 1976).

The governing equations with reference to two phases (alpha and mesomorphic phase) are:

$$d\xi_\alpha / dt = (1 - \xi_\alpha - \xi_m) n_\alpha \ln 2 \left[\int_0^t K_\alpha(T) ds\right]^{n_\alpha - 1} K_\alpha(T) \tag{14}$$

$$d\xi_m / dt = (1 - \xi_\alpha - \xi_m) n_m \ln 2 \left[\int_0^t K_m(T) ds\right]^{n_m - 1} K_m(T) \tag{15}$$

Where α and m indices stand for the alpha monoclinic and the mesomorphic phases respectively. This system of two coupled ordinary differential equations can be integrated with the appropriate initial conditions ($\xi_a=\xi_m=0$ for $t=0$). The integration leads to crystallinity development with time under any temperature history.

Fig. 16a shows a typical *K(T)* curve for the two different phases, and **fig. 16b** outlines the influence of two main parameters, the product of K_0*D (nearly the area under the *K(T)* curve sometimes called crystallizability, Ziabicki, 1976) and the Avrami index *n*. This latter is representative of the sensitivity of the crystallization kinetics to the cooling rate, a larger *n* leads in fact to a faster dependence of final crystallinity on cooling rate, the curves crossover is however always the same, i.e. about one half of the maximum attainable crystallization at an abscissa of K_0*D. The crystallizability is a cooling rate scaling factor of crystallization kinetics; as a matter of fact, a larger value of K_0*D leads to a shift along the abscissa of the curve, i.e. along the cooling rate, such that the larger the crystallizability the more pronounced the material tendency to crystallize.

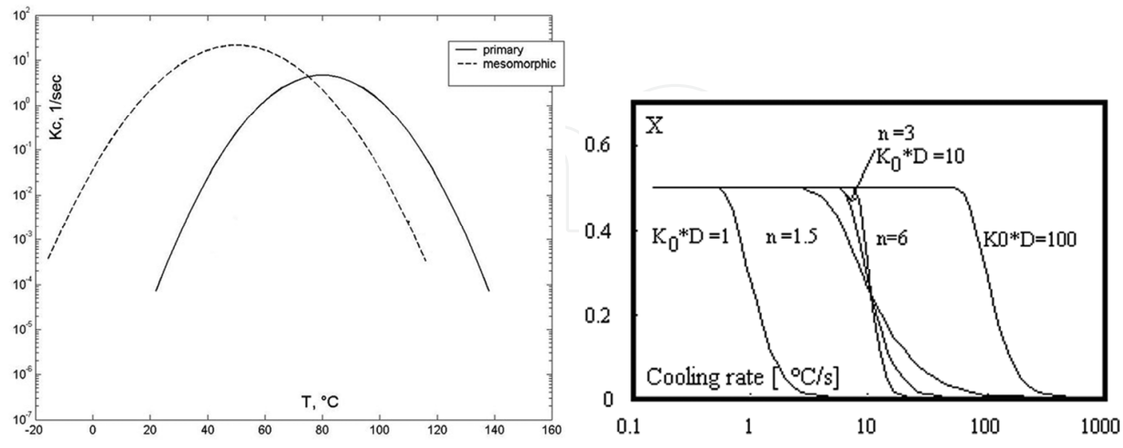

a b

Fig. 16. a. Kinetics constant versus temperature for a and mesomorphic phase; b. Crystallinity volume fraction as a function of cooling rate for various values of n (Avrami index) and K0*D (crystallizability).

Before discussing the results obtained concerning the sensitivity of the cited parameters on polymer composition, it is worth to point out the intrinsic limitations of the approach adopted related to its empirical nature. They depend on the origin of the KAE equation describing the nucleation and growth without diffusivity constraints and without accounting for the possible non isokinetic contribution of each mechanism, with a simple mathematical extension to the non isothermal conditions and finally without accounting for the complexity of crystallization in polymer melts, clearly a multistage process (Strobl, 1997). A slightly different modelling is represented by the so-called "Schneider rate equations" (Schneider et al., 1988); Schneider et al underline that their approach consists in an application of Avrami's (and Tobin's) impingement model leading to a different mathematical and more easy-to-handle formulation, based on a set of differential equations instead of dealing with integral equations. In other words, although their formulation enhances the applicability to process modelling, the physics behind it is completely described by the Avrami model. Therefore the use of Schneider's approach is more advisable when dealing with "non-lumped" problem, to be solved by coupling of transport equations.

All things considered, an analysis of the literature studies on polymer crystallization kinetics shows that the isokinetics approach is the most widely adopted (see the recent review by Pantani et al – Pantani et al., 2005); moreover, the limitations imposed by the isokinetic hypothesis do not weaken the self consistency and the abundance of information here provided. In any case, the limits of the aforementioned approach can be overcome by recalling the original Kolmogoroff's model (which accounts for the number of nuclei per unit volume on spherulitic growth rate) and determining the average radius of spherulites based on geometrical considerations (i.e. counting the number of nuclei), as shown by Zuidema et al. (Zuidema et al., 2001) and Pantani et al. (Pantani et al., 2002). This approach has however some limitations since it can be applied only to conditions where a recognizable spherulitic morphology is formed thus either low cooling rates or conditions where the spherulites are dispersed in a non crystalline matrix as in the case of mesomorphic iPP phase (Piccarolo, 1991). This possible refinement of the analysis is however far beyond the scope of the present work both due to its limitations and to the macroscopic approach adopted aiming to describe crystallization kinetics parameters in the broadest possible range of quiescent solidification conditions, i.e. under conditions emulating, but for the role of orientation and pressure, polymer processing.

4.4 Density data and crystallization kinetics model parameters for various iPPs

Figs. **17.a** and **b** and 18.a and b show a comparison of the density dependence upon cooling rate for the iPP grades studied, whereas **Table 2** reports the crystallization kinetics model parameters calculated by a best fitting procedure not only on the basis of the final monoclinic and mesomorphic content of the quenched samples, taken from the deconvolution of the WAXD patterns, but also accounting for results which provide the time and the temperature at the maxima of the crystallization rate (isothermal tests and DSC measurements) respectively. For this purpose a multiobjective optimization code was adopted.

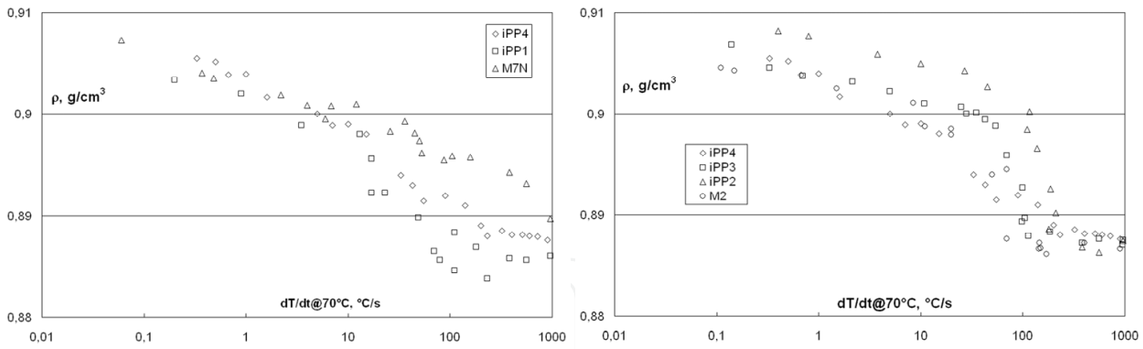

Fig. 17. a.Effect of nucleating agents b.Effect of molecular weight distribution onto the density versus cooling rate behavior.

It should be noticed that **Table 2** reports for the mesomorphic phase a range of values both for the Avrami index *n* and for X_∞. The uncertainty in those parameters is however not critical for the purpose of the present work. As a matter of fact, a variability of *n* between 0.4 and 0.5 reflects into very slight changes in the temperature field in which crystallization takes place; consequently, the influence of this parameter is of minor entity. As for X_∞ of the mesomorphic phase, although its variability could turn into larger changes in the crystallization temperature window, its influence is confined to a cooling rate region in which the crystallization of the alpha phase is very little (very high cooling rates), thus not affecting the alpha phase kinetic parameters.

Material	*monoclinic*						*meso*					
	K_0, sec^{-1}	T_{max}, °C	D, °C	n	X_∞	K_0*D, °Csec^{-1}	K_0, sec^{-1}	T_{max}, °C	D, °C	n	X_∞	K_0*D, °Csec^{-1}
HPB	1.6	82	28	2	0.55	44.8	1.6	57	19	0.4 - 0.5	0.45 - 0.55	30.4
M2	1.4	77.3	33	3.0	0.60	46.2	0.6	40	30			18
M12	2.5	79	30	2.0	0.51	75	3.3	42	31			94
M7N	8.0	82	30	2	0.48	240	n.a.	n.a.	n.a.			n.a
M9	2.0	70	36	3.0	0.53	102	2.0	40	36			72
M6	2.4	66	40	3.0	0.54	96	2.0	40	40			80
M14	40	72	29	3.0	0.40	1160	1.0	40	34			34
M16	1.8	71	33	3.0	0.50	99.4	1.0	40	34			34
iPP1	1.6	82	28	2	0.55	44.8	1.6	57	19			30.4
iPP2	3.5	73	34	2	0.50	255.5	1.5	40	31			60
iPP3	2.7	70	35	2	0.57	189	0.22	40	40			8.8
iPP4	4.5	85	27	2	0.45	121	0.27	53.5	33.8			9.12

Table 2. Crystallization Kinetics Parameters

As for the Avrami index of the crystalline alpha phase, **Table 2** reports values equal to 2.0 or 3.0, due to a slight round-off with respect to the results obtained via simulation. The Avrami index is here intended as a mere fitting parameter, in line with most of the literature concerning polymer crystallization kinetics (see for instance the review of Pantani et al. – Pantani et al., 2002 and the review of Di Lorenzo et al. - Di Lorenzo & Silvestre, 1999), although its exact physical meaning should indicate the dimensionality of growth (namely 3 or 4 for volume filling depending whether nucleation is predetermined of sporadic). In other words, the Avrami index points out only the sensitivity of the crystallization kinetics to the cooling rate, a larger n leads in fact to a faster dependence of final crystallinity on cooling rate, the curves crossover being always the same, i.e. about one half of the maximum attainable crystallization at an abscissa of K_0*D.

Table 2 shows that differences in materials do not appear to be related in a simple way to kinetic parameters. This may be due to the fact that the set of materials investigated in this work, since representative of iPP's of industrial use, does not cover a wide range of fundamental molecular parameters Mw and Mwd. As a matter of fact, the limited range of the molecular parameters here explored probably does not comply with a complete enlightenment of the role played by each single factor onto the crystallization behaviour.

Nevertheless, some information can be drawn from the table summarizing material kinetics behaviour. For example, the so called "crystallizability", i.e. the product K_0*D instead of the two separate kinetic parameters, allows one to discuss the differences in the non isothermal crystallization behaviour in relationship to the materials investigated in this work. The crystallizability, roughly corresponding to area under the kinetic constant curve versus temperature, has the dimension of a cooling rate, and indicates somehow the ability of the polymer to crystallize (Ziabicki, 1976). A comparison of crystallizability values gives a good insight into the influence of molecular parameters on the crystallization kinetics behaviour. For instance, referring to the monoclinic phase only, it can be observed that the smallest value of K_0*D was obtained for the sample without additives having the highest Mw and narrowest Mwd. The highest values of crystallizability are however observed for nucleated iPP's (M7N and M14). All things considered, it should be however underlined that differences in crystallizability below a factor 2-3 cannot be considered reliably assessed by the crystallization kinetics method, due to the intrinsic errors in the evaluation of both K and D throughout the best fitting procedure. If one looks at **fig. 17a**, reporting density as a function of cooling rate for three polymers having similar features (molecular mass and distribution) except for the presence of nucleating agents, one comes to the conclusion that the presence of nucleants shifts the density cut-off towards larger values of cooling rate; as a matter of fact, the calculated crystallizability of the iPP denominated M7N (strongly nucleated) results larger than the one of iPP1 and iPP4.

Higher values of crystallizability are observed when the molecular weight distribution is broader (see for instance materials iPP2 and iPP3). This behaviour is clearly shown in **fig. 17b**, where four polymers with Mwd ranging from 3.5 (M2) to 26 (iPP2) are reported. The observable shift of density cut-off towards larger cooling rate upon increasing Mwd is correctly accompanied by a parallel increase of crystallizability (see **Table 2**).

On the other hand, no direct and obvious correlation may be found to relate crystallizability to Mw. This apparent inconsistency can be reasonably explained by recalling the already mentioned low variability of molecular weights of the iPP grades investigated in this work, related to their "commercial" nature. Consequently, in the light of crystallization behaviour, all the iPP molecular weights listed in **Table 2** have to be considered rather similar, being their difference in molecular weight not sufficient to develop dissimilar crystallization kinetics. Addition of small amounts of ethylene units in the copolymer does not influence significantly any of the kinetic parameters mentioned above, the small changes of the product K_0*D mainly depending on the differences in Mwd and not upon the ethylene content. No significant differences in the product K_0*D may be argued between materials M6, M9 and M16, although the second couple is copolymerized with ethylene. Also the amount of ethylene used in the copolymerization process does not appear to be relevant. These results are confirmed by density data shown in **fig. 18a**.

On the contrary, the couple of nucleated materials (M7N e M14) that basically differ from the others for the addition of ethylene in the latter, show a large difference in the crystallizability, suggesting a synergetic effect of copolymerization with the addition of a nucleating agent on crystallization kinetics. Although the enhancement of chain mobility, which increases with ethylene content, and nucleation are both factors promoting the crystallization kinetics, the source of the synergy is not simple to interpret. The tacticity index does not seam to have a significant influence on the kinetics of monoclinic alpha phase. **Fig. 18b** shows that the density cut-off of M12, with a lower tacticity, is slightly anticipated with respect to the one of MP6; on the other hand, crystallizability of M12 is somehow lower than the one of M6 (see **Table 2**).

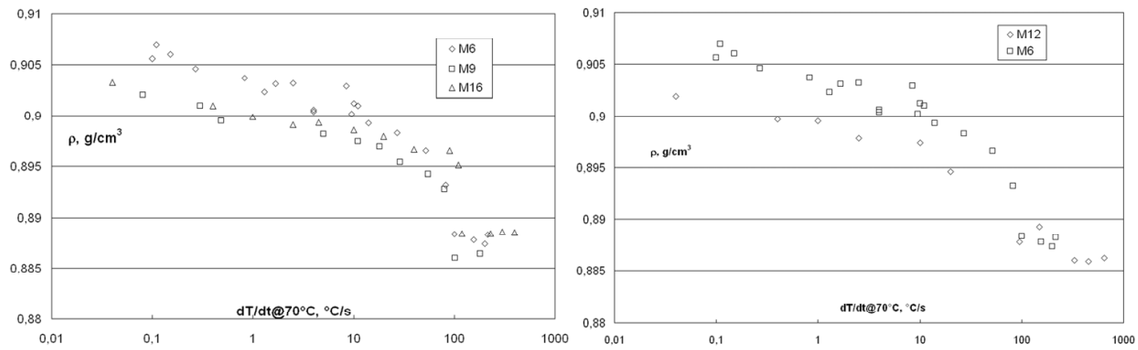

a b

Fig. 18. a.Effect of tacticity b. Effect of ethylene content onto the density cooling rate behavior

Other kinetics parameters of the monoclinic phase are more difficult to be related to molecular parameters. Additionally, their physical meaning is not straightforward with the exception of Avrami index n. This last, in principle, represents the dimensionality of the growth and the kind of nucleation. Experiments, however, rarely well correlate with a value of n in line with the dimensionality of the crystallization process under observation.

Furthermore, the correlation of mesomorphic phase kinetics parameters appears difficult, probably this can be related to the fact that mesomorphic phase determinations are affected by a larger uncertainty due to the broader WAXD peaks characterizing this phase.

With this respect, some recent cooling experiments performed on a nanocalorimeter (De Santis et al., 2007) have shown two distinct crystallization peaks (alpha and mesomorphic

phase) appearing in a quite large range of cooling rates, the crystallization of the alpha taking place up to ca 1000 °C/s. The apparent contradiction with the results here presented (alpha phase disappearing above 200-300 °C/s) may be consistently solved if one considers that the amount of alpha phase formed at high cooling rates is of the order of a few percent, hence below the measure limits of WAXD (around 5%). Secondly, being the sample mass undergoing the DSC cooling run in the nanocalorimeter of the order of a few ng, the enhancement of crystallization due to the "surface effect" (high constraints due to the low sample size with respect to the average radius of giration) must be taken into account. Thirdly, the presence of a mesomorphic phase crystallization peak at room temperature justifies the difficulties encountered in iPP amorphization, as confirmed by the present results where a consistent value of the crystallization kinetic constant of the mesomorphic phase at room temperature is shown (see **Table 2**).

Finally, if one considers that, with a few exceptions, the study was executed on a set of materials of industrial interest, a conclusion can be drawn about the fact that crystallization kinetics are mainly influenced only by the presence of nucleating agents. The influence of copolymerization on crystallization kinetics being relevant only if coupled with nucleation.

5. Conclusion

An experimental route for investigating polymer crystallization over a wide range of cooling rates (from 0.01 up to 1000 °C/s) and pressures (from 0.1 to 40 MPa) is illustrated, using a method that recalls the approach adopted in metallurgy for studying structure development in metals. Two typologies of experimental set-up were used; respectively an apparatus for fast cooling of thin films (100 to 200 mm thick) at various cooling rates under atmospheric pressure and a device (based on a on-purpose modified injection moulding machine) for quenching massive samples (about 1-2 cm^3) under hydrostatic pressure fields.

In both cases ex-situ characterization experiments were carried out to probe the resulting structure, using techniques like density measurements and Wide Angle X-ray Diffraction (WAXD) patterns. The cooling mechanism and the temperature distribution across the sample thickness were analysed. Results show that the final structure is determined only by the imposed thermal history and pressure.

Experimental results of quiescent crystallization at ambient pressure for various grades of isotactic polypropylene (iPP) are reported, showing the reliability of this experimental approach to assess not only quantitative information but also a qualitative description of the crystallization behaviour. In order to thoroughly describe the crystallization kinetics as a function of molecular and operating parameters, the methodological path followed was the preparation of quenched samples of known cooling histories, calorimetric crystallization isotherms tests, Differential Scanning calorimetry (DSC) cooling ramps, Wide Angle X-ray Diffraction (WAXD) measurements and density determination. The WAXD analysis performed on the quenched iPP samples confirmed that during the fast cooling at least a crystalline structure and a mesomorphic one form. The diffractograms were analysed by a deconvolution procedure, in order to identify the relationship between the cooling history and the distribution of the crystalline phases. The whole body of results (including calorimetric ones) provides a wide basis for the identification of a crystallization model suitable to describe solidification in polymer-processing operations, based on the Kolmogoroff-Avrami-Evans non-isothermal approach.

A systematic investigation about the crystallization kinetics under cooling rates typical of polymer processing for several commercial isotactic polypropylene grades was carried out, aiming to highlight the relevance of a number of molecular parameters, including molecular weight and distribution, tacticity, ethylene units content and nucleating agents.

The approach adopted, although the equations used are clearly empirical, is rather general and it surely represents a development with respect to phenomenological procedures describing relationships between structure and processing conditions. In the intention of the work, the kinetic parameters are the connections among such macroscopic observations.

Furthermore, the chapter provides a large amount of consistent experimental data under non-isothermal conditions (cooling rate range from below 0.1 to above 1000°C/s) for a broad set of commercial iPP's so far not extensively reported in literature.

It should be however underlined that he model provides values of K(T) comparable for the different grades, K(T) being the reciprocal of half-crystallization isothermal time regardless the value of the Avrami index. The most influential factor turned out to be the presence of nucleating agents, which shifts toward larger value the material intrinsic "crystallizability" (represented by area under the "bell-shaped" crystallization kinetics constant vs. temperature curve). In particular, the effect of molecular weight does not appear to be very relevant, due to the limited range of molecular weights available in material grades of a "commercial" nature. On the other hand, an increase in the polydispersity index significantly reflects into a parallel increase in crystallizability. Finally, addition of small amounts of ethylene units in the copolymer does not influence the kinetic parameters.

6. References

Alfonso, G. C. & Ziabicki A. (1995). *Coll Polym Sci*, Vol.273, p. 317, ISSN: 0303-402X.

Avrami M. (1939). *J Chem Phys*, Vol.7, p.1103, ISSN: 0021-9606.

Avrami M. (1940). *J Chem Phys*, Vol.8, p.212, ISSN: 0021-9606.

Avrami M. (1941). *J Chem Phys*, Vol.9, p.177, ISSN: 0021-9606.

Bird, R.B.; Stewart, W.E.; & Lightfoot, E.N. (1960). *Transport Phenomena*, Wiley, New York, ISBN-13: 978-0470115398

Brandgrup, J. & Immergut, E. H (1989). *Polymer Handbook*, John Wiley and Sons, ISBN: 0-471-81244-7

Brucato, V.; Crippa, G.; Piccarolo, S. & Titomanlio, G. (1991a). *Polym Eng Sci*, Vol.31, p.1411, ISSN: 1548-2634.

Brucato, V.; Piccarolo, S. & Titomanlio G. (1991b). *Proceedings of European Regional Meeting of the Polymer Processing Society*, Palermo, p.299.

Brucato, V.; Piccarolo, S. & Titomanlio, G. (1993). *Makromol Chem Macrom Symp*, Vol.68, p.245, ISSN: 1022-1360.

Brucato, V.; Piccarolo, S. & Titomanlio, G. (1998). *Int J Form Proc*, Vol.1, No.1, p.35, ISSN: 1292-7775.

Brucato, V.; Piccarolo, S. & La Carrubba, V. (2000). *Int Pol Proc*, Vol.15, No.1, p.103, ISSN: 0930-777X.

Brucato, V.; Piccarolo, S. & La Carrubba, V. (2002). *Chem Eng Sci*, Vol.57, p.4129, ISSN: 0009-2509.

Brucato V.; Kiflie Z., La Carrubba V., Piccarolo S. (2009). *Adv Pol Techn*, Vol.28, No.2, p.86, ISSN: 1098-2329.

Carslaw, H. S. & Jaeger, J. C. (1986). *Conduction of Heat in Solids*, Oxford Science, London, ISBN-13: 978-0198533689.

Chen J.H., Tsai F.C., Nien Y.H. & Yeh P.H. (2005). *Polymer*, Vol.46, p.5680, ISSN: 0032-3861.
Choi, C. & White, J. L. (2000). *Polym Eng Sci*, Vol.40, No.3, p.645, ISSN: 1548-2634.
Ciofalo, M.; Di Piazza, I. & Brucato, V. (198). *Int J Heat Mass Transfer*, Vol.42, p.1157, ISSN: 0017-9310.
Corradini, P.; Petraccone, V.; De Rosa, C. & Guerra, G (1986). *Macromolecules*, Vol.19, p.2699, ISSN: 0024-9297.
De Rosa C.; Auriemma F. & Resconi L. (2005). *Macromolecules*, Vol.38, p.10080, ISSN: 0024-9297.
De Santis F.; Adamovsky S.; Titomanlio G. & Schick C. (2007). *Macromolecules*, Vol. 40, No.25, p.9026, ISSN: 0024-9297.
Di Lorenzo M.L. & Silvestre C. (1999). *Prog Polym Sci*, Vol.24, p.917, ISSN: 0340-255X.
Ding, Z. & Spruiell J. (1996). *J Polym Sci Part B: Polym Phys*, Vol.34, p.2783, ISSN: 1099-0488.
Douillard, A.; Dumazet, Ph.; Chabert, B. & Guillet, J. (1993). *Polymer*, Vol.34, No.8, p.1702, ISSN: 0032-3861
Eder, G. & Janeschitz-Kriegl, H (1997). *Structure development during processing 5: Crystallization*. *Material Science and Technology, vol. 18*; Weinheim: H.E.N. Meijer ed.
Elmoumni, A.; Gonzalez-Ruiz, R.A.; Coughlin, E.B. & Winter H.H. (2005). *Macrom. Chem. Phys.*, Vol.206, p.125, ISSN: 1521-3935.
Evans U.R. (1945). *Trans. Faraday Soc.*, Vol.41, p.365, ISSN: 0956-5000.
Fann, D.M.; Huang, S.K. & Lee, J.Y. (1998). *Pol Eng Sci*, Vol.38, No.2, p.265, ISSN: 1548-2634.
Foresta T., Piccarolo S. & Goldbeck-Wood G. (2001). *Polymer*, Vol.42, p.1167, ISSN: 0032-3861.
Geil, P.H.; Anderson, F.R.; Wunderlich, B. & Arakawa, T. (1964). *J Polym Sci A:Polym Chem,* Vol.2, p.3707, ISSN: 1099-0518.
Gerardi, F.; Piccarolo, S.; Martorana, A. & Sapoundjieva, D. (1997). *Macromol. Chem Phys*, Vol.198, p.3979, ISSN: 1521-3935.
Gobbe, G.; Bazin, M.; Gounot, J. & Dehay, G. (1988). *J Polym Sci B: Polym Phys*, Vol.26, p.857, ISSN: 1099-0488.
Goodfellow Catalogue (1996). *Goodfellow,* Cambridge Limited, p.318.
Guerra, G.; Vitagliano, V.; De Rosa, C.; Petraccone, V. & Corradini, P. (1990). *Macromolecules*, Vol.23, p.1539, ISSN: 0024-9297.
He, J. & Zoller, P. (1994). *J Polym Sci B: Polym Phys*, Vol.32, No.6, p.1049, ISSN: 1099-0488.
Isachenko, V. P.; Ossipova, V. A. & Sukomel A. S., (1987). *Heat Transfer,* MIR, Moscow, ISBN: 089875027X.
Kovarskii, A. (1994). *High-Pressure Chemistry and Physics of Polymers*, CRC Press, ISBN: 9780849342394.
La Carrubba, V.; Brucato, V. & Piccarolo, S. (2000). *Polym Eng Sci*, Vol.40, No.11, p.2430, ISSN: 1548-2634.
La Carrubba, V. (2001). *Polymer Solidification under pressure and high cooling rate, Ph.D. Thesis*, CUES, Salerno, ISBN: ISBN: 88-87030-27-8.
La Carrubba, V.; Brucato, V. & Piccarolo, S. (2002a). *J Polym Sci B: Polym Phys* Vol.40, p.153, ISSN: 0024-9297.
La Carrubba, V.; Briatico, F.; Brucato, V. & Piccarolo, S. (2002b). *Polym Bull*, Vol.49, p.159, ISSN: 0170-0839.
La Carrubba, V.; Piccarolo, S. &Brucato, V. (2007). *J Appl Polym Sci*, Vol.104, p.1358, ISSN: 1097-4628.
Leute, U.; Dollhopf, W. &Liska, E. (1976). *Colloid Polym Sci*, Vol.254, No.3, p.237, ISSN: 0303-402X.
Liangbin, L.; Huang, R.; Ai, L.; Fude, N.; Shiming, H.; Chunmei, W.; Yuemao, Z. & Dong W. (2000). *Polymer*, Vol.41, p.6943, ISSN: 0032-3861.
Luikov, A.V. (1980). *Heat and Mass Transfer*, MIR, Moscow, ISBN 13: 9780080166322.

Marigo, A.; Marega, C.; Causin, V. & Ferrari P. (2004). *J Appl Pol Sci*, Vol.91, p.1008, ISSN: 1097-4628.
Martorana, A.; Piccarolo, S. & Scichilone, F. (1997). *Macromol Chem Phys*, Vol.198, p.597, ISSN: 1521-3935.
Nagasawa, S.; Fujimori, A.; Masuko, T. & Iguchi, M. (2005). *Polymer*, Vol.46, p.5241, ISSN: 0032-3861.
Nakamura, K.; Katayama, K. & Amano T. (1973). *J Appl Pol Sci*, Vol.17, p.1031, ISSN: 1097-4628.
Nakamura, K.; Watanabe, T.; Katayama, K. & Amano T. (1972). *J Appl Pol Sci*, Vol.16, p.1077, ISSN: 1097-4628.
Pantani, R.; Speranza, V.; Coccorullo, I. & Titomanlio, G. (2002). *Macrom Symp*, vol.185, p.309, ISSN: 1521-3900.
Pantani, R.; Coccorullo, I.; Speranza, V. & Titomanlio, G. (2005). *Prog Polym Sci*, Vol.30, p.1185, ISSN: 0079-6700.
Piccarolo, S. (1992). *J Macromol Sci B*, Vol.31, No.4, p.501, ISSN: 0022-2348.
Piccarolo, S.; Saiu, M.; Brucato, V. & Titomanlio, G. (1992a). *J Appl Polym Sci*, Vol.46, p.625, ISSN: 1097-4628.
Piccarolo, S.; Alessi, S.; Brucato, V. & Titomanlio, G. (1992b). *Proceedings of Crystallization of Polymers, a NATO Advanced Research Workshop*, Mons, p.475.
Piccarolo, S. & Brucato, V. (1996). *Proceedings of the PPS12-Annual Meeting*, Sorrento, p.663.
Raab, M.; Scudla, J.; & Kolarik, J. (2004). *European Polymer J*, Vol.40, p.1317, ISSN: 0014-3057.
Sakurai, T.; Nozue, V.; Kasahara, T.; Mizunuma, K.; Yamaguchi, N.; Tashiro, K.; Amemiya, Y. (2005). *Polymer*, Vol.46, p.8846, ISSN: 0032-3861.
Schneider, W.; Koppl, A. & Berger, J. (1988). *Int Pol Proc*, Vol.2, p.151, ISSN: 0930-777X.
Strobl, G. (1997). *The Physics of polymers, Concepts for Understanding Their Structures and Behavior*, Springer, New York, ISBN: 978-3-540-25278-8.
Struik, L.C.E. (1978). *Physical ageing in amorphous polymers and other materials*, Elsevier, Amsterdam, ISBN-13: 978-0444416551.
Tchizmakov, M.B.; Kostantinopolskaja, M.B.; Zubov, Yu.A.; Bakeev, N.Ph.; Kotov, N.M. & Belov, G.P. (1976). *Visokomol Soed*, Vol.A18, p.1121.
Titomanlio, G.; Speranza, V. & Brucato, V. (1997). *Int Polym Proc*, Vol.12, No.1, p.45, ISSN: 0930-777X.
Titomanlio, G.; Piccarolo, S. & Levati, G. (1988a). *J Appl Polym Sci*, Vol.35, p.1483, ISSN: 1097-4628.
Titomanlio, G.; Rallis, A. & Piccarolo, S. (1988b). *Polym Eng Sci*, Vol.29, p.209, ISSN: 1548-2634.
Van Krevelen, W. (1972). *Properties of Polymers*, Elsevier, Amsterdam, ISBN: 978-0-08-054819-7.
Wunderlich, B. & Arakaw, T. (1964). *J Polym Sci Part A: Polym Chem*, Vol.2, p.3697, ISSN: 1099-0518.
Wunderlich, B. (1973). *Macromolecular Physics, Vol. 1*, Academic Press, New York, ISBN-13: 978-0127656014.
Wunderlich, B. (1976). *Macromolecular Physics, Vol. 2*, Academic Press: New York, ISBN-13: 978-0127656021.
Wunderlich, B. (1980). *Macromolecular Physics, Vol. 3*, Academic Press: New York, ISBN-13: 978-0127656038.
Wunderlich, B. & Davison T. (1969). *J Polym Sci Part A:Polym Chem*, Vol.7, p.2043, ISSN: 1099-0518.
Ziabicki, A. & Alfonso, G.C. (1994). *Coll Polym Sci*, Vol.272, p.1027, ISSN: 0303-402X.
Zimmermann, H.J. (1993). *J Macromol Sci-Phys*, Vol.B32, p.141, ISSN: 0022-2348.
Ziabicki, A. (1976). *Fundamentals of Fibre Formation*, Wiley, London, ISBN: 0-471-98220-2.
Zuidema, H.; Peters, W.M.P. & Meijer H.E.H. (2001). *Macrom Theory Simul*, Vol.10, p.447, ISSN: 1521-3919.
Zoller, P. (1979). *J Appl Polym Sci*, Vol.23, No.4, p.1051, ISSN: 1097-4628.

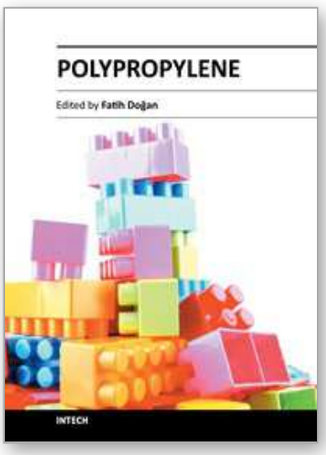

Polypropylene

Edited by Dr. Fatih Dogan

ISBN 978-953-51-0636-4

Hard cover, 500 pages

Publisher InTech

Published online 30, May, 2012

Published in print edition May, 2012

This book aims to bring together researchers and their papers on polypropylene, and to describe and illustrate the developmental stages polypropylene has gone through over the last 70 years. Besides, one can find papers not only on every application and practice of polypropylene but also on the latest polypropylene technologies. It is also intended in this compilation to present information on polypropylene in a medium readily accessible for any reader.

How to reference

In order to correctly reference this scholarly work, feel free to copy and paste the following:

Valerio Brucato and Vincenzo La Carrubba (2012). Solidification of Polypropylene Under Processing Conditions - Relevance of Cooling Rate, Pressure and Molecular Parameters, Polypropylene, Dr. Fatih Dogan (Ed.), ISBN: 978-953-51-0636-4, InTech, Available from: http://www.intechopen.com/books/polypropylene/solidification-of-polypropylene-under-processing-conditions-relevance-of-cooling-rate-pressure-a

INTECH
open science | open minds

InTech Europe
University Campus STeP Ri
Slavka Krautzeka 83/A
51000 Rijeka, Croatia
Phone: +385 (51) 770 447
Fax: +385 (51) 686 166
www.intechopen.com

InTech China
Unit 405, Office Block, Hotel Equatorial Shanghai
No.65, Yan An Road (West), Shanghai, 200040, China
中国上海市延安西路65号上海国际贵都大饭店办公楼405单元
Phone: +86-21-62489820
Fax: +86-21-62489821

IntechOpen